

Article

Comparative Untargeted Metabolic Profiling of Different Parts of *Citrus sinensis* Fruits via Liquid Chromatography–Mass Spectrometry Coupled with Multivariate Data Analyses to Unravel Authenticity

Sherif M. Afifi ^{1,2,*}, Eman M. Kabbash ³, Ralf G. Berger ⁴ , Ulrich Krings ⁴  and Tuba Esatbeyoglu ^{2,*} ¹ Pharmacognosy Department, Faculty of Pharmacy, University of Sadat City, Sadat City 32897, Egypt² Department of Food Development and Food Quality, Institute of Food Science and Human Nutrition, Gottfried Wilhelm Leibniz University Hannover, Am Kleinen Felde 30, 30167 Hannover, Germany³ Phytochemistry Department, National Organization for Drug Control and Research, Giza 12622, Egypt⁴ Institute of Food Chemistry, Gottfried Wilhelm Leibniz University Hannover, Callinstraße 5, 30167 Hannover, Germany

* Correspondence: sherif.afifi@fop.usc.edu.eg (S.M.A.); esatbeyoglu@lw.uni-hannover.de (T.E.)

Abstract: Differences between seven authentic samples of *Citrus sinensis* var. Valencia peel (albedo and flavedo) and juices from Spain and Uruguay, in addition to a concentrate obtained from Brazil, were investigated by untargeted metabolic profiling. Sixty-six metabolites were detected by nano-liquid chromatography coupled to a high-resolution electrospray-ionization quadrupole time-of-flight mass spectrometer (nLC-ESI-qTOF-MS) belonging to phenolic acids, coumarins, flavonoid glycosides, limonoids, terpenes, and fatty acids. Eleven metabolites were detected for the first time in *Citrus sinensis* and identified as citroside A, sinapic acid pentoside, apigenin-C-hexosyl-O-pentoside, chrysoeriol-C-hexoside, di-hexosyl-diosmetin, perilloside A, gingerol, ionone epoxide hydroxy-sphingene, xanthomicrol, and coumaryl alcohol-O-hexoside. Some flavonoids were completely absent from the juice, while present most prominently in the *Citrus* peel, conveying more industrial and economic prospects to the latter. Multivariate data analyses clarified that the differences among orange parts overweighed the geographical source. PCA analysis of ESI(−)-mode data revealed for hydroxylinoleic acid abundance in flavedo peel from Uruguay the most distant cluster from all others. The PCA analysis of ESI(+)-mode data provided a clear segregation of the different *Citrus sinensis* parts primarily due to the large diversity of flavonoids and coumarins among the studied samples.

Keywords: albedo; flavedo; concentrate; juice; orange; metabolomics; flavonoids; coumarins

Citation: Afifi, S.M.; Kabbash, E.M.; Berger, R.G.; Krings, U.; Esatbeyoglu, T. Comparative Untargeted Metabolic Profiling of Different Parts of *Citrus sinensis* Fruits via Liquid Chromatography–Mass Spectrometry Coupled with Multivariate Data Analyses to Unravel Authenticity. *Foods* **2023**, *12*, 579. <https://doi.org/10.3390/foods12030579>

Academic Editors: Noelia Castillejo Montoya and Lorena Martínez-Zamora

Received: 22 December 2022

Revised: 18 January 2023

Accepted: 18 January 2023

Published: 29 January 2023



Copyright: © 2023 by the authors. Licensee MDPI, Basel, Switzerland. This article is an open access article distributed under the terms and conditions of the Creative Commons Attribution (CC BY) license (<https://creativecommons.org/licenses/by/4.0/>).

1. Introduction

Citrus trees bear some of the most popular fruits and are grown globally for food, medicinal and other industrial applications, with a total annual production of nearly 85 million tons [1]. Various species of *Citrus* genus are valuable, such as *C. medica* (citron), *C. limon* (lemon), *C. aurantium* (sour orange), *C. reticulata* (mandarin, tangerine), *C. paradisi* (grapefruit), *C. clementina* (clementine) and *C. sinensis* (sweet orange) [2]. They are either consumed as fresh fruits or after processing to juices, beverage products, and jams, with the peel being the main by-product of processing. Anatomically, the fruit consists of two parts—the outer peel and the pulp with juice sac glands [2]. The peel main parts include the outer pigmented flavedo with parenchymatous cells and cuticle, and the white albedo part lying beneath the flavedo [3]. Different plant parts find wide application in many countries in recipes to treat stomach disorders, skin inflammation, cough, muscular pain, and nausea, as well as being used as a slimming agent [4].

Phytochemical investigations have revealed the presence of bioactive coumarins (i.e., bergamottin, scopoletin, and umbelliferone), flavonoids (i.e., rutin, quercetin, and

kaempferol), limonoids (i.e., limonin and nomilin), and acridone alkaloids (i.e., citruscridone and citrussinine-I) in *Citrus* plants [5]. Dietary fiber, minerals, carotenoids, and phenolic phytoconstituents, i.e., phenolic acids, flavanones, and polymethoxylated flavones, were all detected in orange peel [6]. *Citrus sinensis* var. Valencia fruits revealed superiority as an excellent source of phenolics, flavonoids and ascorbic acid compared to var. Mandarina and some grapefruits grown in Cyprus [7]. Another study on var. Valencia pointed out that the flavedo part had highest vitamin C, flavones and carotenoid content, while the albedo part was the main source of flavanones and phenolics [8].

Moreover, previous clinical and animal studies have demonstrated that certain *Citrus* metabolites have antioxidant, anti-inflammatory, cytotoxic, antimicrobial, antiallergic and antiplatelet aggregation activities [9]. The metabolites in *Citrus* varieties influence their unique qualities, such as taste, appearance, and the supposed health benefits. Quantitative and qualitative differences in these metabolites are commonly affected by the cultivation environment and *Citrus* variety [10] and also vary significantly from one part to another within the *Citrus* fruit.

Although there is a wide variety of *Citrus* fruits that were intensely investigated for their metabolic composition [11], comparative studies of metabolite profiles within different fruit parts are limited. Because metabolite variability and modification are affected by the plant's adaptation to physiological, pathological, and diverse chemical stimuli, metabolomics enables quantitative investigation of these dynamic changes [12]. In-depth food analyses help to uncover discriminatory biomarkers, identify various pathways, find therapeutic targets, and discover new potential drug leads by evaluating and verifying the major variations in metabolite profiling [13].

Metabolite profiling by mass spectrometry is regarded as the most powerful analytical tool. Among the most recent detection techniques are: high-performance liquid chromatography–diode array detection (HPLC-DAD), ultra-high-performance liquid chromatography coupled to triple quadrupole mass spectrometry (UHPLC-QqQ-MS/MS), and ultra-performance liquid chromatography/quadrupole time-of-flight mass spectrometry (UPLC-QTOF-MS/MS) [14]. The analysis of the orange peel matrix has also been performed via HPLC-UV-ESI-MS/MS (high-performance liquid chromatography coupled with ultraviolet and electrospray ionization mass spectrometry) [6]. The current technique involves the use of nano-high-performance liquid chromatography (n-LC) coupled to high-resolution MS to provide fast metabolite analysis of orange peel, to the best of our knowledge, for the first time on a high sensitivity level. Previous studies have been performed via state-of-the-art nano-liquid chromatography–ESI–MS/MS technology to only separate chiral naringenin in *Citrus* pulp and peel [15].

By adding multivariate data analysis (MVA) techniques, a large-scale metabolomics dataset is presented in this study to provide a detailed insight into *C. sinensis* secondary metabolites. The use of MVA enables accurate specimen to specimen comparison and highlights distinctive traits [16].

The aim of this work was to investigate the differences in secondary metabolite composition in different parts of *C. sinensis* presenting the first comparative insights into metabolite profiles derived from various parts of Valencia orange fruits collected from different countries. A detailed identification of metabolites in different *C. sinensis* parts was considered together with an untargeted metabolic profile for the edible part and the peel as the main by-product during fruit processing.







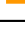
2. Materials and Methods

2.1. Orange Samples and Chemicals

Valencia oranges (*C. sinensis*) from Spain and Uruguay, provided by Symrise (Holzminden, Germany) as depicted in Table 1, were cleaned and squeezed to obtain the juice, then flavedo and albedo were manually stripped by a fruit peeler. After that, all orange samples, including a Brazilian orange concentrate acquired from Symrise, were lyophilized and separately ground to fine powder by a mill rotor cyclone (Tecnal, Piracicaba, Brazil,

TE-651/2). Comminuted orange samples were stored at $-80\text{ }^{\circ}\text{C}$ until subsequent analysis. All chemicals and solvents were purchased from Sigma Aldrich (Steinheim, Germany).

Table 1. Source of the different *Citrus sinensis* (var. Valencia) specimens used in the analysis.

Code	Orange Part	Country
AS 	Albedo peel	Spain
AU 	Albedo peel	Uruguay
CB 	Juice concentrate	Brazil
FS 	Flavedo peel	Spain
FU 	Flavedo peel	Uruguay
JS 	Juice	Spain
JU 	Juice	Uruguay

2.2. Metabolite Mass Fingerprinting

Orange specimens (2 mg), extracted by 1 mL methanol, were spiked with $4\text{ }\mu\text{g mL}^{-1}$ hesperidin followed by sonication for 30 min, then centrifugation for 20 min at $15,000\times g$ to eliminate any leftover debris. Solid-phase extraction was applied to each extract using a C_{18} cartridge (JT Baker, Phillipsburg, NJ, USA) as previously reported [17]. The resulting extracts were injected into a nano-LC system EASY-nLC II (Bruker, Bremen, Germany) equipped with a reversed phase column ($150\times 0.1\text{ mm}$, particle size $3\text{ }\mu\text{m}$; Michrom Bioresources, Auburn, CA, USA) coupled to maXis impact quadrupole-time of-flight (qTOF) MS (Bruker, Bremen, Germany). A captive nano-spray ionization was operated in the negative and positive ion modes under conditions as previously reported [18]. Identification of metabolite mass fingerprints was carried out using exact parent ion masses as well as retention data, reference literature, fragmentation patterns, and the Phytochemical Dictionary of Natural Products Database (<https://dnp.chemnetbase.com/> accessed on (16 March 2022)). Semi-quantification was based on the integrated peak areas of each compound after normalization to internal standard. Aiming at comparing the relative abundance of a given compound in the seven different samples, the determination of absolute concentrations by an external calibration of every compound was not required. Three independent replicates of each orange specimen were analyzed in parallel to evaluate the biological variance.

2.3. Multivariate Data Analyses (MVA)

Modeling viz. principal component analysis (PCA) and orthogonal projection to latent structures-discriminant analysis (OPLS-DA) was applied to a metabolite dataset of MS abundances produced by nLC-MS either in the negative or positive ion mode via the SIMCA-P+ 13.0 software package (Umetrics, Umeå, Sweden) to pinpoint various markers characterizing each group declared with correlation (pcor) and covariance (p). The iterative permutation testing and diagnostic indices, viz. R^2 and Q^2 values, were used to assess the validity of models, while all variables were mean centered and Pareto scaled.

3. Results and Discussion

3.1. Metabolite Identification via nLC-ESI-MS/MS Analysis

nLC-ESI-MS/MS analyses (Figure 1) of *Citrus* samples resulted in the identification of 66 metabolites, categorized into seven classes: phenolic acids, terpenes, limonoids, coumarins, flavonoids, fatty acids and nitrogenous compounds. The elution order of metabolites followed a sequence of decreasing polarity, whereby phenolic acids eluted first, followed by coumarins, flavonoid glycosides, limonoids, free aglyca and fatty acids. Samples were analyzed in both the negative and positive ionization modes to provide a greater coverage of the metabolome. Fatty acids and flavonoids were preferentially ionized under negative ionization conditions, while coumarins, limonoids and nitrogenous compounds showed better ionization in the positive mode. The list of identified compounds

along with their retention time, characteristic molecular and fragment ions and occurrence is presented in Table 2.

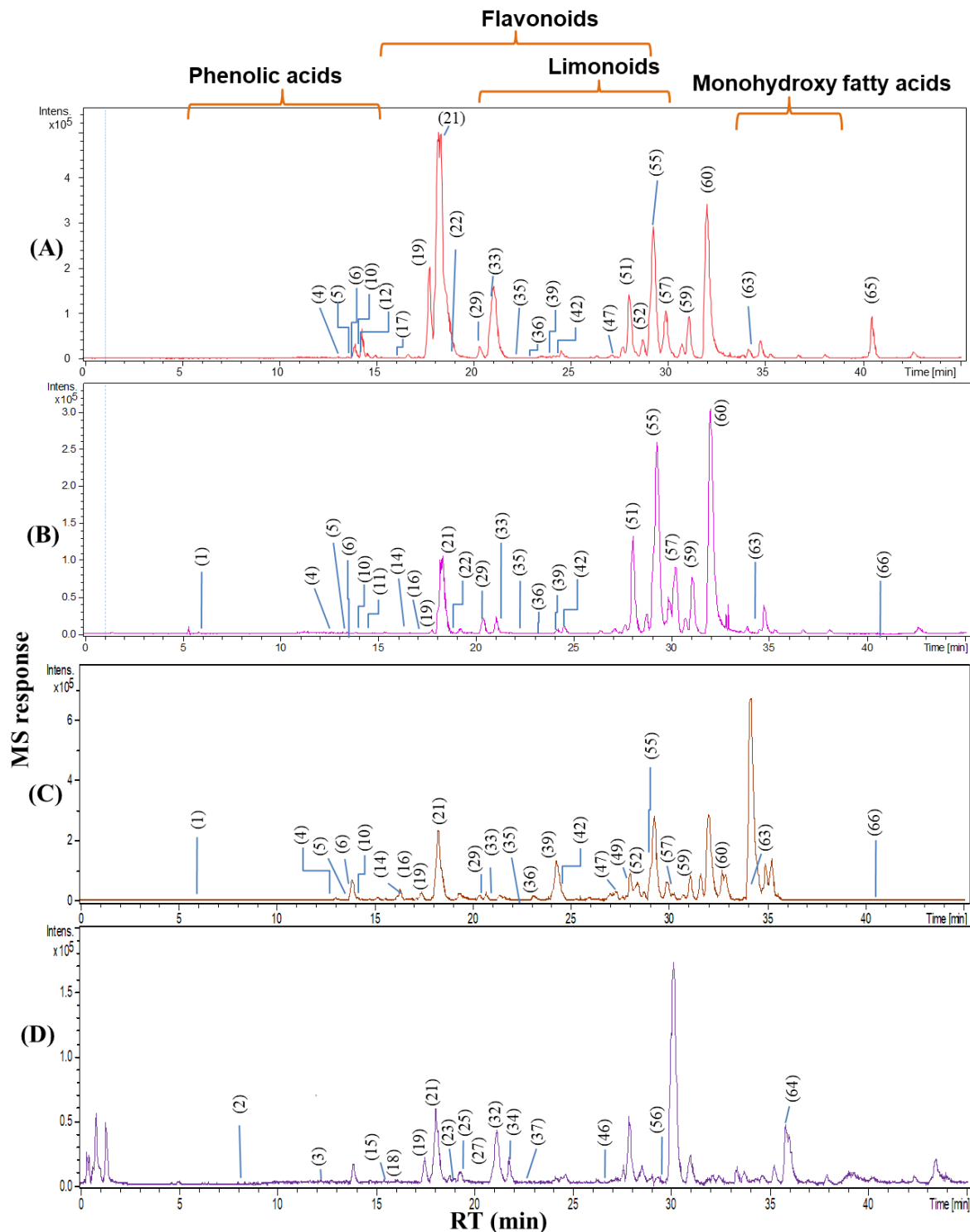


Figure 1. Representative nLC-MS base peak chromatogram of orange parts extracted by methanol on negative ionization (A) albedo from Uruguay, (B) orange concentrate from Brazil, (C) flavedo from Uruguay and on positive ionization, and (D) juice from Uruguay. For peak numbers, refer to Table 2.

3.1.1. Identification of Organic Acids and Phenolics

A number of organic acids were eluted in the first part of the nLC-ESI-MS/MS-chromatogram, as revealed from their MS spectral data. In the analyzed *Citrus* samples, the

most representative phenolic and organic acids were citric, ferulic, sinapic acids and their glycosides. Peak 1—for peak numbers refer to Table 2— $[(M-H)^- m/z 191.0189 (C_6H_7O_7)^-]$ was identified as citric acid previously reported in *Citrus limon* ethanolic extract [19]. Peaks 6 and 8 (Suppl. Figure S1), $[(M-H)^- m/z 355.103 (C_{16}H_{19}O_9)^-]$ were annotated as ferulic acid hexoside and sinapic acid pentoside, respectively. Having the same molecular formula; peak 6 yielded a main fragment ion at $m/z 193 [M-H-162 (\text{hexose})^-]$ relative to ferulic acid, while peak 8 showed a fragment ion at $m/z 223 [M-H-132 (\text{pentose})^-]$ relative to sinapic acid. Sinapic acid pentoside was detected for the first time in all of the examined *Citrus* samples except *Citrus sinensis* juice obtained from Uruguay (JU). In addition, citric acid was absent in the albedo of both suppliers (AS: albedo from Spain, and AU: albedo from Uruguay), while sinapoyl hexoside was absent in the juice (JS: juice from Spain, and JU: juice from Uruguay). Peak 17 $[(M-H)^- m/z 311.1139 (C_{15}H_{19}O_7)^-]$ with product ion at $m/z 161$ corresponding to negatively ionized hexose, was annotated as coumaryl alcohol-*O*-hexoside, first time to be reported in all *Citrus* samples. Peak 55 $[(M-H)^- m/z 293.1763 (C_{17}H_{25}O_4)^-]$ was a major constituent detected in all analyzed samples and identified as gingerol, a pungent principle previously detected in the peel of *Citrus reticulata* [20], but detected for the first time in *Citrus sinensis* and most prominent in albedo from Uruguay and juice from Spain (AU and JS). Ferulic and *p*-coumaric acid were major hydroxycinnamic acids detected in both free and bound form in the methanolic extracts of bitter orange (*Citrus microcarpa*) peel [6].

3.1.2. Identification of Coumarins

Peak 11 $[(M-H)^- m/z 205.0504 (C_{11}H_9O_4)^-]$ yielded fragment ions at $m/z 175 [M-H-30 (C_2H_6)]^-$ and $m/z 101$ corresponding to the loss of CO_2 from the pyrone ring, and was identified as citropten, the most abundant coumarin in *Citrus* (Suppl. Figure S2) [19]. Peak 9 $[(M-H)^- m/z 175.0392 (C_{10}H_7O_3)^-]$ was identified as methoxycoumarin and detected in all *Citrus* samples. Peak 26 $[(M-H)^- m/z 367.0668 (C_{16}H_{15}O_{10})^-]$ showed a characteristic fragment ion at $m/z 191 [M-H-176 (\text{glucuronyl})^-]$ was identified as scopoletin-*O*-glucuronide. The flavedo part from Uruguay showed the highest level of the identified coumarins. This finding was in accordance with results previously reported by Liu et al. (2017) showing that the highest coumarin content was found in the flavedo part among different studied *Citrus* cultivars [21], conveying a particular interest regarding the presumed anticancer and antidiabetic effects of this part.

Table 2. Metabolites annotated in various orange samples via nLC -ESI-MS/MS using both the positive and negative ionization modes.

No.	Rt (min)	Compound Name	Chemical Class	[M−H] [−] / [M + H] ⁺	Molecular Formula	Mass Error	MS/MS frag.	Ref.	AS	AU	CB	FS	FU	JS	JU
1.	5.7	Citric acid	Organic acid	191.0189	C ₆ H ₇ O ₇ [−]	4.3	111, 87	[19]	-	-	++	+	+	++	++
2.	11.1	Feruloylagmatine	Cinnamic acid amide	307.177	C ₁₅ H ₂₃ N ₄ O ₃ ⁺	1.7	264, 177		++	++	+	+	-	+	+
3.	13.0	Hydroxy-phenyl-valeric acid- <i>O</i> -sulphate	Sulphate ester	275.0607	C ₁₁ H ₁₅ O ₆ S ⁺	8.4	195		+	-	+	+	++	+	+
4.	13.2	Dihydroxymegastigmadienone - <i>O</i> -hexoside (Citroside A)	Terpene	385.1860	C ₁₉ H ₂₉ O ₈ [−]	0.8	223, 153	[22]	++	+	+	+	++	-	-
5.	13.9	Sinapoyl hexoside	Phenolic acid	385.1141	C ₁₇ H ₂₁ O ₁₀ [−]	−1.8	223, 190	[19]	++	+	+	+	++	-	-
6.	13.9	Ferulic acid hexoside	Phenolic acid	355.1030	C ₁₆ H ₁₉ O ₉ [−]	0.0	193, 175, 160	[19]	++	++	++	++	++	+	++
7.	13.7	Citropten	Coumarin	205.0504	C ₁₁ H ₉ O ₄ [−]	1.1	175, 101	[19]	+	+	+	+	++	+	+
8.	13.9	Sinapic acid pentoside	Phenolic acid	355.1037	C ₁₆ H ₁₉ O ₁₀ [−]	−0.7	223, 205	[23]	++	+	+	++	+	+	-
9.	13.9	Methoxycoumarin	Coumarin	175.0392	C ₁₀ H ₇ O ₃ [−]	0.2	-	[24]	+	+	+	+	+	+	+
10.	14.0	Sinapic acid	Phenolic acid	223.0607	C ₁₁ H ₁₁ O ₅ [−]	0.2	-	[19]	++	++	++	+	++	+	+
11.	14.2	Di-hexosyl-diosmetin	Flavone	625.1757	C ₂₈ H ₃₃ O ₁₆ ⁺	−1	-	[25]	+	+	+	++	++	-	-
12.	14.3	Naringenin- <i>O</i> -hexoside	Flavanone	433.1145	C ₂₁ H ₂₁ O ₁₀ [−]	1.2	271	[26]	++	++	-	+	-	-	-
13.	14.7	Limononic acid	Limonoid degradation	183.1024	C ₁₀ H ₁₅ O ₃ [−]	1.6	-		++	+	+	+	++	-	+
14.	13.2	Methyl epijasmone	Fatty acid degradation	223.1337	C ₁₃ H ₁₉ O ₃ [−]	1.3	-	[27]	++	++	+	+	++	+	+
15.	16.4	Apigenin-di- <i>C</i> -hexoside	Flavone	595.1654	C ₂₇ H ₃₁ O ₁₅ ⁺	1.5	385	[26]	+	+	+	++	++	+	+
16.	16.5	Apigenin-di- <i>O</i> -hexoside	Flavone	593.1502	C ₂₇ H ₂₉ O ₁₅ [−]	8.6	431, 269	[26]	+	-	+	+	++	-	-
17.	16.6	Coumaryl alcohol- <i>O</i> -hexoside	Cinnamyl alcohol glycoside	311.1139	C ₁₅ H ₁₉ O ₇ [−]	1.1	269, 161		+	+	+	+	++	+	+
18.	16.8	Apigenin- <i>C</i> -hexosyl- <i>O</i> -pentoside	Flavone	563.1408	C ₂₆ H ₂₇ O ₁₄ [−]	0.3	311	[28]	-	-	+	+	++	+	+
				565.1550	C ₂₆ H ₂₉ O ₁₄ ⁺	0.3									
19.	17.5	Naringenin- <i>O</i> -hexosyldeoxyhexoside	Flavanone	579.1720	C ₂₇ H ₃₁ O ₁₄ [−]	1.0	271								
				581.1867	C ₂₇ H ₃₃ O ₁₄ ⁺	−0.5	419, 273	[29]	++	++	++	+	+	+	+
20.	17.6	Chrysoeriol- <i>C</i> -hexoside	Flavone	463.1238	C ₂₂ H ₂₃ O ₁₁ ⁺	−0.1	343	[26]	+	+	+	++	++	+	+
21.	18.2	Hesperidin (Hesperetin- <i>O</i> -hexosyldeoxyhexoside)	Flavanone	609.1833	C ₂₈ H ₃₃ O ₁₅ [−]	−2.2	301	[29]	++	++	++	++	++	++	+
				611.1971	C ₂₈ H ₃₅ O ₁₅ ⁺	0.1	-								
22.	18.3	Limonin-hexoside	Limonoid	649.2507	C ₃₂ H ₄₁ O ₁₄ [−]	0.7	-	[30]	+	+	+	+	+	+	+
23.	18.7	Hesperetin- <i>O</i> -deoxyhexoside	Flavanone	449.1625	C ₂₂ H ₂₅ O ₁₀ ⁺	−0.4	303	[19]	++	+	-	+	+	-	-
24.	19.1	Azelaic acid	Dicarboxylic acid	187.0969	C ₉ H ₁₅ O ₄ [−]	2.1	169, 125		+	+	+	+	+	+	+
25.	19.3	Deacetylnomilin	Limonoid	473.2167	C ₂₆ H ₃₃ O ₈ ⁺	−1.7	455, 411, 161		++	+	+	+	+	+	+
26.	19.4	Scopoletin- <i>O</i> -glucuronide	Coumarin	367.0668	C ₁₆ H ₁₅ O ₁₀ [−]	−0.1	191		+	+	+	+	++	+	+
27.	20.2	Pyridoxamine phosphate	Vitamin B6 phosphate	249.0614	C ₈ H ₁₄ N ₂ O ₅ P ⁺	−8.4	169, 81	[31]	+	+	++	+	+	+	+
28.	20.3	Unknown	Alkaloid	368.1921	C ₁₅ H ₃₀ NO ₉ ⁺	−13	-		+	+	-	++	++	+	-
29.	20.4	Decatrienoic acid	Fatty acid	165.0913	C ₁₀ H ₁₃ O ₂ [−]	−5.0	-		+	+	+	+	+	+	+
30.	21.0	Sakuranetin- <i>O</i> -hexosyl- <i>O</i> - deoxyhexoside	Flavanone	595.2020	C ₂₈ H ₃₅ O ₁₄ ⁺	−1.2	433, 287	[28]	++	++	-	+	+	-	-

Table 2. Cont.

No.	Rt (min)	Compound Name	Chemical Class	[M–H] [–] / [M + H] ⁺	Molecular Formula	Mass Error	MS/MS frag.	Ref.	AS	AU	CB	FS	FU	JS	JU
31.	20.7	Hydroxyhexadecanedioic acid	Fatty acid	303.2171	C ₁₆ H ₃₁ O ₅ [–]	1.1	259, 214	[32]	+	-	-	+	++	-	-
32.	20.9	Sakuranetin-O-hexosyl deoxyhexoside	Flavanone	593.1835	C ₂₈ H ₃₃ O ₁₄ [–]	1.7	285		+	+	++	++	++	++	+
33.	21.1	Nomilin-hexoside	Limonoid	595.2018	C ₂₈ H ₃₅ O ₁₄ ⁺	-1.5		[19]	++	++	+	+	+	++	+
34.	21.2	Sakuranetin	Flavanone	693.2723	C ₃₄ H ₄₅ O ₁₅ [–]	5.9	159		++	++	+	+	+	+	+
35.	22.5	Perilloside A	Terpene	285.0770	C ₁₆ H ₁₃ O ₅ [–]	2.5	255	[29]	++	++	+	+	+	+	+
36.	23.0	Trihydroxy-octadecadienoic acid (trihydroxy-linoleic acid)	Fatty acid	287.1042	C ₁₆ H ₁₅ O ₅ ⁺	0.7	237		++	+	+	++	+	+	-
37.	23.7	Hydroxy-sphingene	Ceramide	313.1651	C ₁₆ H ₂₅ O ₆ [–]	-0.3	-	[33]	++	+	+	++	+	+	-
38.	23.9	Linoleamide	Fatty acid amide	327.2175	C ₁₈ H ₃₁ O ₅ [–]	0.9	-	[28]	+	+	+	+	++	+	+
39.	24.1	Trihydroxy-octadecenoic acid	Fatty acid	316.2827	C ₁₈ H ₃₈ NO ₃ ⁺	-6.1	-	[34]	+	+	++	+	+	+	-
40.	24.2	Demethylnobiletin	Methoxy-flavone	280.2677	C ₁₈ H ₃₄ NO ⁺	1.4	-	[35]	+	-	-	+	-	++	-
41.	24.3	Methyl dihydrojasmonate	Organic acid	329.2333	C ₁₈ H ₃₃ O ₅ [–]	1.5	-		+	+	+	+	++	+	+
42.	17.7	Naringenin	Flavanone	389.1234	C ₂₀ H ₂₁ O ₈ ⁺	-0.8	-	[36]	-	-	-	+	++	-	-
43.	26.1	Nobiletin	Methoxy-flavone	225.1496	C ₁₃ H ₂₁ O ₃ [–]	-0.4	-		+	+	+	+	+	+	+
44.	18.5	Hesperetin	Flavanone	271.0606	C ₁₅ H ₁₁ O ₅ [–]	0.0	-	[37]	+	+	++	++	+	++	++
45.	26.5	Unknown	Methoxy-flavone	403.1385	C ₂₁ H ₂₃ O ₈ ⁺	-1.2	388, 373, 342	[38]	+	+	+	++	++	-	-
46.	27.2	Tangeretin	Methoxy-flavone	301.0717	C ₁₆ H ₁₃ O ₆ [–]	0.9	-	[29]	++	++	+	+	+	+	+
47.	27.7	Methyl-dodecadienoate	Fatty acid ester	403.1568	C ₂₅ H ₂₃ O ₅ ⁺	7.4	373		-	-	+	+	++	+	+
48.	27.8	Unknown	Alkaloid	373.1312	C ₂₀ H ₂₁ O ₇ ⁺	6.7	343, 312	[39]	+	+	+	+	+++	+	+
49.	27.9	Dimethylkaempferol	Methoxy-flavone	209.1548	C ₁₃ H ₂₁ O ₂ [–]	2.4	-		+	+	+	+	+	++	+
50.	28.0	γ-Lactone hydroxy-dodecenedioic acid methyl ester	Fatty acid ester	272.1862	C ₁₄ H ₂₆ NO ₄ ⁺	-1.8	255, 237		++	+	+	+	+	+	+
51.	28.1	Limonin	Limonoid	313.0718	C ₁₇ H ₁₅ O ₆ [–]	1.9	163, 117	[40]	-	+	+	++	++	-	-
52.	28.3	Methylimonexic acid	Limonoid	253.1443	C ₁₈ H ₁₅ O ₇ [–]	0.0	209		+	+	+	+	+	+	+
53.	28.4	Dihydroxytrimethoxyflavone (xanthomicrol)	Methoxy-flavone	469.1869	C ₂₆ H ₂₉ O ₈ [–]	1.5	-	[30]	++	+	+	+	+	+	+
54.	29.0	Tetramethoxyflavone (Tetra-O-methylscutellarein)	Methoxy-flavone	471.2018	C ₂₆ H ₃₁ O ₈ ⁺	0.2	453, 161	[30]	++	+	-	+	+	+	+
55.	29.2	Gingerol	Phenylpropen-oid polyketide	515.1925	C ₂₇ H ₃₁ O ₁₀ [–]	1.6	469, 229	[41]	++	+	-	+	+	+	+
56.	29.5	Heptamethoxyflavone	Methoxy-flavone	343.0826	C ₁₈ H ₁₅ O ₇ [–]	0.2	298, 270, 242		+	-	+	++	++	-	-
57.	29.9	Ionone epoxide	Terpene	343.1201	C ₁₉ H ₁₉ O ₆ ⁺	7.2	313, 282		+	+	+	++	++	-	-
58.	28.7	Hydroxy-tetradecatrienoyl glycerol	Acylglycerol	293.1763	C ₁₇ H ₂₅ O ₄ [–]	3.8	193	[20]	+	++	+	+	+	++	+
59.	31.6	Dihydroxyoctadecadienoic acid	Fatty acid	455.1313	C ₂₂ H ₂₄ O ₉ Na ⁺	-1.1	433	[42]	-	-	+	+++	++	-	-
60.	32.0	N-Phenylacetyl glycine	Nitrogenous compound	433.1511	C ₂₂ H ₂₅ O ₉ ⁺	-4.1	403		+	+	+	+	+	+	+
				207.1392	C ₁₃ H ₁₉ O ₂ [–]	-3.4	-	[43]	+	+	+	+	+	+	+
				311.1857	C ₁₇ H ₂₇ O ₅ [–]	-2.2	-		+	+	+	+	++	+	+
				311.2225	C ₁₈ H ₃₁ O ₄ [–]	1.2	211, 171, 129		+	+	+	++	++	+	+
				194.0821	C ₁₀ H ₁₂ NO ₃ [–]	0.8	-		+	+	++	+	+	++	+

Table 2. Cont.

No.	Rt (min)	Compound Name	Chemical Class	$[M-H]^- / [M+H]^+$	Molecular Formula	Mass Error	MS/MS frag.	Ref.	AS	AU	CB	FS	FU	JS	JU
61.	32.5	Hydroxy-oxohexadecanoic acid	Fatty acid	285.2069	$C_{16}H_{29}O_4^-$	0.7	-	[44]	++	++	+	+	+	+	+
62.	32.5	Hydroxylinolenic acid	Fatty acid	293.2115	$C_{18}H_{29}O_3^-$	-2.4	275, 235	[45]	+	+	-	+	++	-	-
63.	34.1	Hydroxyoctadecadienoic acid (Hydroxylinoleic acid)	Fatty acid	295.2276	$C_{18}H_{31}O_3^-$	1.6	-		+	+	+	+	++	+	+
64.	35.7	Heptyl caffeate	Cinnamic acid ester	301.1421	$C_{16}H_{22}O_4Na^+$	1.7	279		+	+	-	++	++	+	++
65.	39.1	Erucamide (Docosenamide)	Fatty acid amide	279.1600	$C_{16}H_{23}O_4^+$	-3.3			-	-	+	+	-	++	-
66.	40.5	Linoleic acid	Fatty acid	338.3428	$C_{22}H_{44}NO^+$	-3.1	321	[35]	-	-	+	+	-	++	-
				279.2326	$C_{18}H_{31}O_2^-$	1.3	-	[45]	+	++	+	+	+	+	+

AS: Albedo from Spain; AU: Albedo from Uruguay; CB: concentrate from Brazil; FS: Flavedo from Spain; FU: Flavedo from Uruguay; JS: Juice from Spain; JU: Juice from Uruguay. Signs (-, +, ++ and +++) indicate relative semi-quantification of each compound based on the integrated peak areas of the total ion; - = absent, + = present, ++ = present in higher amount, and +++ = present in highest amount.

3.1.3. Identification of Flavonoids

A total of 22 flavonoid derivatives were identified with better ionization in the negative ion mode as a result of their rapid deprotonation ability. Peak 20 [(M + H)⁺ *m/z* 463.1238 (C₂₂H₂₃O₁₁)⁺], with a fragment ion at *m/z* 343 [M + H – 120]⁺ was identified as chrysoeriol-C-hexoside. Peak 15 [(M + H)⁺ *m/z* 595.1654 (C₂₇H₃₁O₅)⁺] showed a fragment ion at *m/z* 385 [M + H – 120 – 90]⁺, indicating di-C-hexoside, and was identified as apigenin-di-C-hexoside (vicenin-2). Vicenin-2 was previously identified in the peels and edible pulp of *C. aurantiifolia*, and *C. unshiu* [46]. Both flavones, chrysoeriol-C-hexoside and vicenin-2, were detected in all the analyzed samples with relatively high concentration in flavedo peel of both suppliers.

Peaks 12 and 19 showed the same deprotonated aglycone fragment ion at *m/z* 271, and were identified as naringenin derivatives. Peak 12 [(M – H)[–] *m/z* 433.1145 (C₂₁H₂₁O₁₀)[–]] with MS² fragment at *m/z* 271 [M – H – 162 (hexose)][–] was identified as naringenin-O-hexoside. Peak 19 [(M + H)⁺ *m/z* 581.1867 (C₂₇H₃₃O₁₄)⁺] showed fragment ions (Suppl. Figure S3) at *m/z* 419 [M + H – 162 (hexose)]⁺ followed by successive loss of a deoxyhexose at *m/z* 273 [M + H – 162 (hexose) – 146 (deoxyhexose)]⁺, while peak 31 showed a base signal at *m/z* 273.0756 [M + H – 308 (rutinose)]⁺ indicating that both carbohydrate moieties were linked through an -O-glycosidic bond [47]. Thus, peak 19 was identified as naringenin-O-hexosyldeoxyhexoside.

Likewise, Peaks 16 and 18 showed the same deprotonated fragment ion at *m/z* 269 indicating apigenin derivatives. Peak 16 [(M – H)[–] *m/z* 593.1502 (C₂₇H₂₉O₁₅)[–]] with MS² fragments at *m/z* 431 [M – H – 162 (hexose)][–] and *m/z* 269 [M – H – 162 (hexose) – 162 (hexose)][–], indicating successive losses of two hexose moieties, was identified as apigenin-di-O-hexoside previously detected in different *Citrus* species [26]. Peak 18 [(M – H)[–] *m/z* 563.1408 (C₂₆H₂₇O₁₄)[–]]/[(M + H)⁺ *m/z* 565.1550 (C₂₆H₂₉O₁₄)⁺] was a mixed O-C flavone, with characteristic fragment ion at *m/z* 311 [M – H – 120 (cross ring cleavage of C-hexosyl) – 132 (pentose)][–]. It was identified as apigenin-C-hexosyl-O-pentoside, first reported in *Citrus sinensis* (Suppl. Figure S4). In the studied samples, flavedo peel from Uruguay was found more enriched in apigenin derivatives, while naringenin derivatives were found most abundant in the albedo part of both suppliers.

Peaks 30 showed deprotonated fragment ion at *m/z* 285, indicating sakuranetin derivatives. Peak 30 showed fragment ions at *m/z* 433 [M + H – 162 (hexose)]⁺ followed by successive loss of a deoxyhexose at *m/z* 287 [M + H – 162 (hexose) – 146 (deoxyhexose)]⁺. Thus, peak 30 was identified as sakuranetin-O-hexosyl-O-deoxyhexoside.

Peak 21 [(M – H)[–] *m/z* 609.1833 (C₂₈H₃₃O₁₅)[–]]/[(M + H)⁺ *m/z* 611.1971 (C₂₈H₃₅O₁₅)⁺] showed a MS² fragment ion in the negative ionization mode at *m/z* 301 [M – H – 308 (rutinose)][–] and was the main flavanone glycoside identified in all samples (Suppl. Figure S5). It was annotated as hesperidin, previously reported as the main flavanone in the peel of *Citrus sinensis* L. varieties, which suffers dramatic losses in filtered peel juice due to its relatively low water solubility [48]. Hesperidin is well known for its supposed effects on health including antimicrobial, anticancer, antihypertensive and antiulcer effects, thus attracting medicinal interest to orange peel [49].

A number of polymethoxy flavones (PMF) were identified in the studied samples being more readily ionized in the positive ion mode than in the negative mode. In general, the PMF MS² spectra had characteristic fragments at [M + H – *n*CH₃]⁺, [M + H – 2CH₃ – CO]⁺ and [M + H – 2CH₃ – H₂O]⁺ [50]. Peak 43 [(M + H)⁺ *m/z* 403.1385 (C₂₁H₂₃O₈)⁺], peak 46 [(M + H)⁺ *m/z* 373.1312 (C₂₀H₂₁O₇)⁺] and peak 53 [(M – H)[–] *m/z* 343.0826 (C₁₈H₁₅O₇)[–]] showed typical fragmentation patterns for PMF and were identified as nobiletin, tangeretin and dihydroxytrimethoxy-flavone, respectively. Xanthomicrol (dihydroxytrimethoxy-flavone) was previously isolated from *Citrus sudachi* [51] but reported herein for first time in *C. sinensis*. Likewise, peak 54 [(M + H)⁺ *m/z* 343.1201 (C₁₉H₁₉O₆)⁺] and peak 56 [(M + H)⁺ *m/z* 433.1511 (C₂₂H₂₅O₉)⁺] were annotated as tetra-O-methylscutellarein and heptamethoxyflavone, respectively. In addition to xanthomicrol, other hydroxylated PMFs were detected as demethylnobiletin (peak 40), and dimethylkaempferol (peak 49). Gen-

erally, PMFs exhibited extensive range of biological actions, i.e., antiatherogenic, and anti-inflammation activities [52]. However, hydroxylated PMFs revealed potent antineoplastic effects against various cancer types [53]. Flavedo peel from Uruguay was the richest part in methoxy flavones in contrast to the juice from both suppliers. The flavedo extracts of various *Citrus* fruits encompassed flavanone glycosides (poncirin, hesperidin, neohesperidin, dydimin, naringin, narirutin, and neoeriocitrin), flavonol glycosides (rutin), and flavone glycosides (diosmin, rhoifolin, and isorhoifolin) [6].

3.1.4. Identification of Limonoids and Terpenes

Limonoids are tetranortriterpenoids, found extensively in Rutaceae and Meliaceae [54]. They are widely distributed in different *Citrus* fruits, such as grapefruit (*Citrus paradisi*), sweet orange (*Citrus sinensis*), sour orange (*Citrus aurantium*), lemon (*Citrus limon*) and lime (*Citrus aurantifolia*) [55]. Water-insoluble limonoid aglycones are mainly distributed within seeds and peels. In contrast, the water-soluble limonoid glycosides are more abundant within juices and pulps [56]. In the studied *Citrus* samples, limonoids occur in significant amounts as aglycone and glycoside forms. Peak 25 [(M + H)⁺ *m/z* 473.2167 (C₂₆H₃₃O₈)⁺] showed MS² fragments at *m/z* 455 [M + H – 18 (H₂O)]⁺, 411 [M + H – 62 (CH₂O₃)]⁺ and the characteristic ion for *Citrus* limonoids at *m/z* 161 attributed to the furan ring bound to a lactone ring moiety [57] and was identified as deacetylnomilin (Suppl. Figure S6). It was found more abundant in the peel than in juice or concentrate; this may be related to its relatively low water solubility. Peak 51 with protonated and deprotonated molecular ions [(M + H)⁺ *m/z* 471.2018 (C₂₆H₃₁O₈)⁺]/[(M – H) *m/z* 469.1869 (C₂₆H₂₉O₈)[–]] showed a fragment ion *m/z* 453 [M + H – 18 (H₂O)]⁺ and the characteristic fragment ion for *Citrus* limonoids at *m/z* 161. It was identified as limonin, a well-known limonoid that possesses various biological, mainly anti-inflammatory activities [58]. Limonin was detected in more abundant content in albedo from Spain (AS), suggestive to have a slightly bitter taste compared to albedo from Uruguay (AU) upon providing a likely sustainable source of food additive [59].

Terpenes are important for plant aroma and flavor playing key roles in fruit quality, plant defense and pollinator attraction. A total of three terpenes was detected ionized most preferentially in the negative ionization mode, from which a gluco-conjugated megastigmadienone was identified as peak 4 [(M – H)[–] *m/z* 385.1860 (C₁₉H₂₉O₈)[–]] known as citroside A. Its MS² fragments showed the characteristic fragment ion at *m/z* 223 [M – H – 162 (hexose)][–] relative to the loss of a hexose moiety. Citroside A was reported previously to be a precursor of damascenone and 3-hydroxydamascone, two important industrial flavor compounds. It has been reported in *Citrus unshiu* leaves, *Solanum quitoense* leaves [60] and *Gynostemma pentaphyllum* [61]. Herein it was detected for the first time in the peel of *Citrus sinensis* being more prominent in albedo peel from Spain and flavedo peel from Uruguay (AS and FU). A number of monoterpenes belonging to different classes were identified: Peak 35 [(M – H) *m/z* 313.1651 (C₁₆H₂₅O₆)[–]] was a monoterpene glycoside identified as perilloside A, detected for the first time in *Citrus* and found most prominent in albedo and flavedo peel from Spain (AS and FS), suggestive to be a marker to distinguish between peels from Spain and Uruguay. Peak 57 [(M – H)[–] *m/z* 207.1392 (C₁₃H₁₉O₂)[–]] was an apo-carotenoid monoterpene identified as ionone epoxide, a flavoring substance with a fruity and woody flavor previously identified in many foods, such as apricot, raspberry, tea and lemon balm [43].

3.1.5. Identification of Fatty Acids and Fatty Acid Amides

Saturated and unsaturated fatty acids in addition to low molecular mass amide compounds were detected in several orange peel compartments. For details, refer to Supplementary Materials [28,35,44].

3.1.6. Identification of Nitrogenous Compounds

Other metabolites containing nitrogen were detected at trace levels. For details, refer to Supplementary Materials [34].

3.2. Multivariate Data Analyses of Orange Samples

The datasets encompassed a total of 42 nLC-ESI-MS/MS runs (seven different orange samples with three biological replicates each in both the negative and positive ionization modes). Thus, unsupervised and supervised multivariate data analyses were adopted to simplify interpretation of such complex datasets allowing better biomarkers characterization and sample classification [62]. Principal component analysis (PCA), as an unsupervised approach, was reported to evaluate the variance within various samples involving no prior knowledge of the datasets [63]. Table 1 shows the color-coded source of the *Citrus sinensis* specimens compared.

PCA on negative ionization runs as depicted in Figure 2A–C for all orange samples was illustrated by PC1 and PC2 accounting for 87% of the total variance (Figure 2A). Along PC1, there was a clear separation between flavedo specimens from Spain (FS) and Uruguay (FU), while the latter was distinguished from the other samples and located at upper right quadrant with positive score values, suggesting the impact of geographical source based on their metabolites. The albedo samples were positioned at the lower right quadrant, whereas juice samples were located at upper left quadrant with negative PC1 values. Conversely, orange concentrate from Brazil (CB) appeared near the origin (Figure 2A). The respective loading plot demonstrated that mono-methoxy flavonoids, i.e., hesperetin and sakuranetin along with hydroxy-oxohexadecanoic acid were found more abundant in albedo specimens (Figure 2B). On the other hand, hydroxylinoleic acid was major contributor to flavedo from Uruguay (FU) being the most distant data point. Naringenin was responsible for the clustering of orange juice of both suppliers and flavedo from Spain (FS) in the upper left quadrant, while *N*-phenylacetyl glycine was more abundant in juice from Spain (JS) and orange concentrate (CB). The dendrogram of HCA (Hierarchical clustering analysis), as depicted in Figure 2C, revealed that flavedo from Uruguay (FU) represented one cluster, whereas the other cluster was divided into albedo specimens at one sub-group and the other sub-group encompassed the remaining samples.

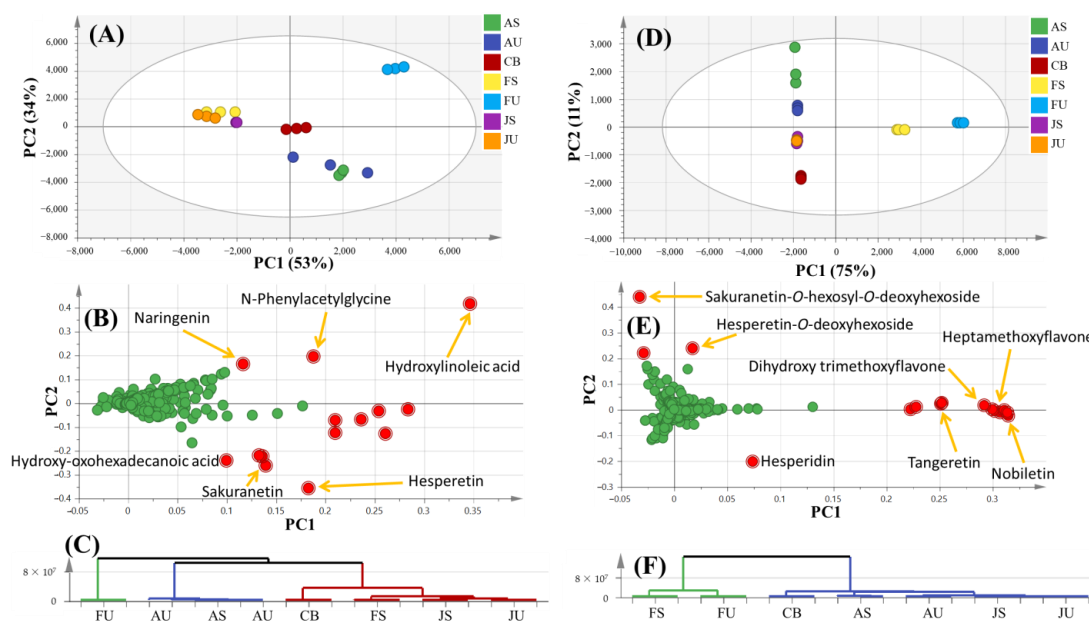


Figure 2. MS-based PCA of all orange samples ($n = 3$) negative ionization (A) score plot, (B) relevant loading plot and (C) HCA; positive ionization (D) score plot, (E) relevant loading plot and (F) HCA. AS: Albedo from Spain; AU: Albedo from Uruguay; CB: concentrate from Brazil; FS: Flavedo from Spain; FU: Flavedo from Uruguay; JS: Juice from Spain; JU: Juice from Uruguay.

Likewise, PCA on positive ionization as illustrated in Figure 2D–F revealed 86% of the total variance, albeit with better segregation (Figure 2D) compared to its negative ionization counterpart. Particularly, all replicates from each orange sample were tightly clustered indicating the superb reproducibility of the experimental analysis in both the negative and positive ionization modes. In agreement with the previous PCA model, flavedo from Uruguay (FU) was also the most distant group. Flavedo specimens showed positive score values separable from other orange parts, while orange juice and concentrate had negative score values. Albedo from both countries (AU and AS) was separated in the upper left quadrant. The respective loading plot (Figure 2E) demonstrated high levels of nobiletin, tangeretin, dihydroxytrimethoxyflavone and heptamethoxyflavone in flavedo samples. Albedo specimens were enriched in sakuranetin-*O*-hexosyl-*O*-deoxyhexoside and hesperetin-*O*-deoxyhexoside, whereas high levels of hesperidin were observed in orange juice and concentrate. The HCA dendrogram, as depicted in Figure 2F, revealed that the flavedo from both suppliers represented one cluster, while the other cluster included the remaining orange parts.

OPLS-DA (orthogonal projection to latent structures-discriminant analysis) as a supervised approach was reported to possess a great potentiality maximizing the segregation of overlapping sample groups by identifying chemical determinants [64]. Being the most distant cluster, flavedo from Uruguay (FU) was further subjected to OPLS-DA against all other specimens (Figure 3) to assess sample discrimination with p value less than 0.001. The first OPLS model on negative ionization (Figure 3A) exhibited 0.96 model predictability (Q²) and 97% total variance (R²). The relevant loading S-plot showed that FU included abundant levels of hydroxylated fatty acids, i.e., hydroxylinoleic, trihydroxylinoleic, and dihydroxyoctadecadienoic acids (Figure 3B). Conversely, the second OPLS model on positive ionization (Figure 3C) exhibited 0.62 model predictability (Q²) and 72% total variance (R²). The relevant loading S-plot revealed that nobiletin, dihydroxytrimethoxyflavone, demethylnobiletin and tangeretin were detected in higher levels in FU (flavedo from Uruguay) (Figure 3D). Then, several OPLS models were constructed (Suppl. Figures S7–S10) with p value less than 0.001 to assess chemical determinants in orange parts derived from the various countries. Hence, a model of flavedo from Uruguay (FU) against its counterpart from Spain (FS) was performed (Suppl. Figure S7). On negative mode, OPLS model (Suppl. Figure S7A) revealed the enrichment of flavedo from Uruguay (FU) in hydroxyl-linoleic acid, dimethylkaempferol, apigenin-di-*O*-hexoside and citropten (Suppl. Figure S7B). Notably, hydroxyl fatty acids other than hydroxylinoleic acid did not appear in this model, which was attributed to their similar levels present in both samples. Conversely, OPLS model in positive mode (Suppl. Figure S7C) exhibited the enrichment of flavedo from Uruguay (FU) in nobiletin, demethylnobiletin, and tangeretin, whereas heptamethoxyflavone was abundant in FS (Suppl. Figure S7D). Another OPLS model was performed with albedo from Uruguay (AU) versus its counterpart from Spain (AS) (Suppl. Figure S8). OPLS model in negative ionization (Suppl. Figure S8A) demonstrated the particular abundance of naringenin-*O*-hexoside and linoleic acid in albedo from Uruguay (AU), while hesperetin, sakuranetin and hydroxy-oxohexadecanoic acid were found more abundant in albedo from Spain (Suppl. Figure S8B). In positive ionization, the OPLS model (Suppl. Figure S8C) showed significantly higher levels of glycosyl flavonoids, i.e., sakuranetin-*O*-hexosyl-*O*-deoxyhexoside, limonin and hesperetin-*O*-deoxyhexoside in AS (albedo from Spain) (Suppl. Figure S8D). Further and for better discrimination assessment of orange juices derived from various sources, the OPLS model in negative mode (Suppl. Figure S9A) revealed abundant levels of *N*-phenylacetyl glycine, nomilinhexoside and gingerol in orange juice from Spain (JS) (Suppl. Figure S9B). Lastly, the OPLS model including orange juice from both suppliers and orange concentrate from Brazil (CB) was implemented in positive mode (Suppl. Figure S10A). The relevant loading plot (Suppl. Figure S10B) showed that hesperidin, hydroxy-sphinganine and pyridoxamine phosphate amounted for the major metabolites in orange concentrate (CB). The obvious segregation between orange juice from Uruguay (JU) and Spain (JS) was ascribed to the

abundance of heptyl caffeate in the former, while the later was enriched in nomilinhexoside and sakuranetin-*O*-hexosyl-deoxyhexoside.

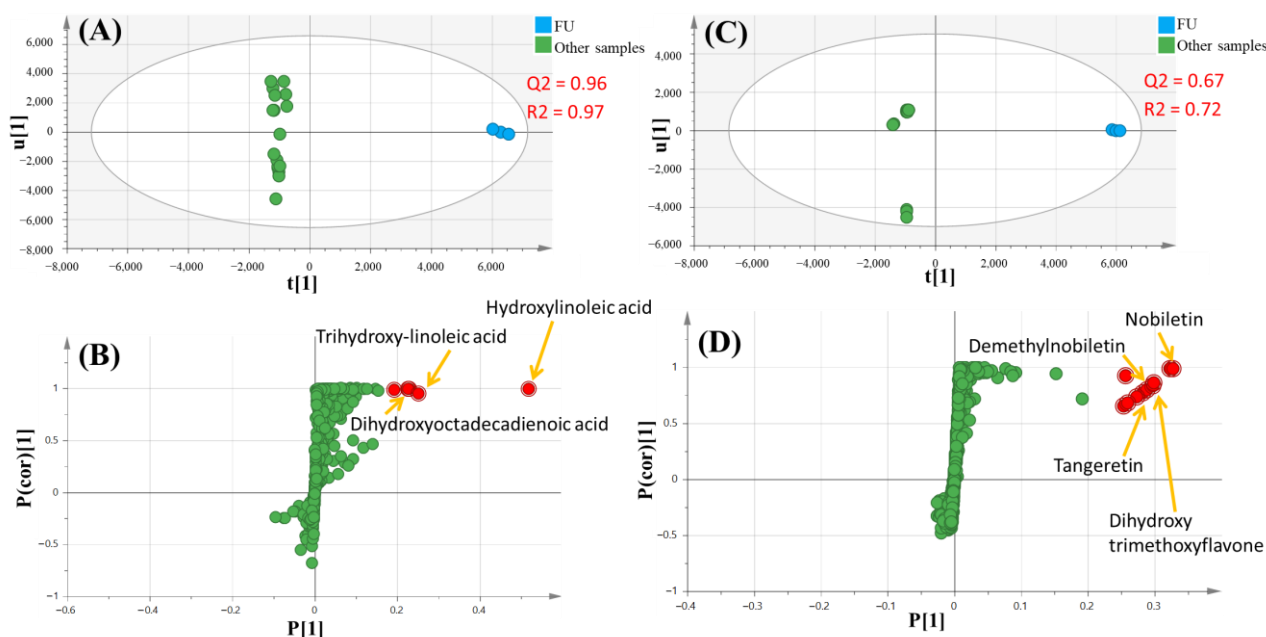


Figure 3. MS-based OPLS of flavedo from Uruguay (FU) against all other samples negative ionization (A) score plot and (B) relevant loading S-plot; positive ionization (C) score plot and (D) relevant loading S-plot.

4. Conclusions

In this study, the metabolites in the orange peels (albedo and flavedo parts) together with the juice and concentrate from different suppliers were systematically analyzed and identified using state-of-the-art nLC-ESI-MS/MS-based, widely non-targeted metabolome analysis. A total of 66 metabolites were annotated, 37 of which were compounds shared by all samples. Furthermore, 29 differential metabolites were detected, 15 of which were mainly flavonoids and completely absent from the juice. A total of eleven metabolites were detected for the first time in *Citrus sinensis*: citroside A, sinapic acid pentoside, di-hexosyl-diosmetin, apigenin-*C*-hexosyl-*O*-pentoside, chrysoeriol-*C*-hexoside, perilloside A, hydroxy-sphinganine, xanthomicrol, coumaryl alcohol-*O*-hexoside, gingerol and ionone epoxide. The annotation of the novel metabolites warrants in-depth functional genomic mining to identify their various biosynthetic pathways. Comparing different fruit parts, a number of flavonoids with proposed preventive therapies against some diseases, i.e., naringenin-*O*-hexoside, hesperetin-*O*-deoxyhexoside, sakuranetin-*O*-hexosyl-*O*-deoxyhexoside, and demethylnobiletin, were completely absent from the juices, but present most prominent in the peel. *Citrus* peel is thus considered a renewable bio-resource of functional foods. In addition, hesperetin-*O*-deoxyhexoside, sakuranetin-*O*-hexosyl-*O*-deoxyhexoside and hydroxylinolenic acid were detected only in albedo and flavedo of both suppliers, albeit absent in orange juices and concentrate, suggestive to be a distinctive marker for orange peel and to increase the potential transform of *Citrus* by-products into valuable food ingredients, nutraceuticals, and perhaps even pharmaceuticals.

The comprehensive nLC-ESI-MS/MS metabolic profiling followed by multivariate data analyses suggested that the differences between orange parts were much more obvious than the geographical source. Generally, albedo was richer in mono-methoxylated flavonoids, while flavedo was richer in poly-methoxylated flavonoids and hydroxylated fatty acids. Moreover, further research is required to more accurately evaluate the effectiveness, the toxicity, and the mechanism of action of many PMFs as well as to increase their bioavailability by using readily accessible and appropriate drug delivery vehicles.

Further analysis of more orange samples from other sources has yet to be evaluated to obtain a bigger picture of the entire respective population of orange samples. In addition, other factors, i.e., seasonal variation, storage conditions and agricultural practices may be assessed using the same platform.

Supplementary Materials: The following supporting information can be downloaded at: <https://www.mdpi.com/article/10.3390/foods12030579/s1>, Figure S1: MS² Spectra of A: ferulic acid hexoside [M–H][−] 355.1024, C₁₆H₁₉O₉[−], B: sinapic acid pentoside [M–H][−] 355.1025, C₁₆H₁₉O₉[−]. Figure S2: MS² spectra of ciropten [M–H][−] 205.0495, C₁₁H₉O₄[−]. Figure S3: MS² spectra of naringenin-O-hexosyldeoxyhexoside [M–H][−] 579. 1687 C₂₇H₃₁O₁₄[−]. Figure S4: MS² spectra of apigenin-C-hexoside-O-pentoside [M–H][−] 563.1416, C₂₆H₂₇O₁₄[−]. Figure S5: MS² spectra of hesperidin [M–H][−] 609.1832, C₂₈H₃₃O₁₅[−]. Figure S6: MS² spectra of deacetylnomilin [M + H]⁺ 473.222, C₂₆H₃₃O₈⁺. Figure S7: MS-based OPLS of flavedo from Uruguay (FU) against that from Spain (FS) (*n* = 3) negative ionization (A) score plot and (B) relevant loading S-plot; positive ionization (C) score plot and (D) relevant loading S-plot. Figure S8: MS-based OPLS of albedo from Uruguay (AU) against that from Spain (AS) (*n* = 3) negative ionization (A) score plot and (B) relevant loading S-plot; positive ionization (C) score plot and (D) relevant loading S-plot. Figure S9: MS-based OPLS of orange juice from Uruguay (JU) against that from Spain (JS) (*n* = 3) negative ionization (A) score plot and (B) relevant loading S-plot. Figure S10: MS-based OPLS of orange juice from Uruguay (JU) and Spain (JS) and orange concentrate (CB) (*n* = 3) positive ionization (A) score plot and (B) relevant loading plot. References [63,64] are cited in the supplementary materials.

Author Contributions: Conceptualization, S.M.A. and T.E.; methodology, S.M.A., E.M.K., U.K., R.G.B. and T.E.; validation, S.M.A. and E.M.K.; formal analysis, S.M.A., U.K. and R.G.B.; investigation, S.M.A., E.M.K., U.K., R.G.B. and T.E.; writing—original draft preparation, S.M.A. and E.M.K.; writing—review and editing, S.M.A., E.M.K., U.K., R.G.B. and T.E.; funding acquisition, R.G.B. and T.E. All authors have read and agreed to the published version of the manuscript.

Funding: This research project was partially supported by the German academic exchange program (DAAD; German Egyptian Research Short-Term Scholarship—GERSS program). The publication of this article was funded by the Open Access Fund of Leibniz Universität Hannover.

Data Availability Statement: Not applicable.

Acknowledgments: We thank Silke Hillebrand from Symrise (Holzminden, Germany) for providing the *Citrus* samples.

Conflicts of Interest: The authors declare no conflict of interest.

References

- Paw, M.; Begum, T.; Gogoi, R.; Pandey, S.K.; Lal, M. Chemical Composition of *Citrus limon* L. Burmf Peel Essential Oil from North East India. *J. Essent. Oil Bear. Plants* **2020**, *23*, 337–344. [[CrossRef](#)]
- Favela-Hernández, J.M.J.; González-Santiago, O.; Ramírez-Cabrera, M.A.; Esquivel-Ferriño, P.C.; Camacho-Corona, M.D.R. Chemistry and pharmacology of *Citrus sinensis*. *Molecules* **2016**, *21*, 247. [[CrossRef](#)] [[PubMed](#)]
- Suri, S.; Singh, A.; Nema, P.K. Current applications of citrus fruit processing waste: A scientific outlook. *Appl. Food Res.* **2022**, *2*, 100050. [[CrossRef](#)]
- Olaiya, C.; Adigun, A. Chemical manipulation of tomato growth and associated biochemical implications on flavonoid, lycopene and mineral contents. *Afr. J. Plant Sci.* **2010**, *4*, 167–171.
- Peixoto, J.S.; Comar, J.F.; Moreira, C.T.; Soares, A.A.; De Oliveira, A.L.; Bracht, A.; Peralta, R.M. Effects of *Citrus aurantium* (bitter orange) fruit extracts and p-synephrine on metabolic fluxes in the rat liver. *Molecules* **2012**, *17*, 5854–5869. [[CrossRef](#)]
- Singh, B.; Singh, J.P.; Kaur, A.; Singh, N. Phenolic composition, antioxidant potential and health benefits of citrus peel. *Food Res. Int.* **2020**, *132*, 109114. [[CrossRef](#)]
- Goulas, V.; Manganaris, G.A. Exploring the phytochemical content and the antioxidant potential of *Citrus* fruits grown in Cyprus. *Food Chem.* **2012**, *131*, 39–47. [[CrossRef](#)]
- Escobedo-Avellaneda, Z.; Gutiérrez-Urbe, J.; Valdez-Fragoso, A.; Torres, J.A.; Welte-Chanes, J. Phytochemicals and antioxidant activity of juice, flavedo, albedo and comminuted orange. *J. Funct. Foods* **2014**, *6*, 470–481. [[CrossRef](#)]
- Fattahi, J.; Hamidoghli, Y.; Fotouhi, R.; Ghasemnejad, M.; Bakhshi, D. Assessment of fruit quality and antioxidant activity of three citrus species during ripening. *South-West. J. Hortic. Biol. Environ.* **2011**, *2*, 113–128.
- Zhao, X.J.; Xing, T.T.; Li, Y.F.; Jiao, B.N. Analysis of phytochemical contributors to antioxidant capacity of the peel of Chinese mandarin and orange varieties. *Int. J. Food Sci. Nutr.* **2019**, *70*, 825–833. [[CrossRef](#)] [[PubMed](#)]

11. Salonia, F.; Ciacciulli, A.; Poles, L.; Pappalardo, H.D.; La Malfa, S.; Licciardello, C. New plant breeding techniques in citrus for the improvement of important agronomic traits. A Review. *Front. Plant Sci.* **2020**, *11*, 1234. [[CrossRef](#)] [[PubMed](#)]
12. Farag, M.A.; Fathi, D.; Shamma, S.; Shawkat, M.S.A.; Shalabi, S.M.; El Seedi, H.R.; Afifi, S.M. Comparative metabolome classification of desert truffles *Terfezia claveryi* and *Terfezia boudieri* via its aroma and nutrients profile. *LWT* **2021**, *142*, 111046. [[CrossRef](#)]
13. Ammar, N.M.; Hassan, H.A.; Ahmed, R.F.; AE, G.E.-G.; Abd-ElGawad, A.M.; Farrag, A.R.H.; Farag, M.A.; Elshamy, A.I.; Afifi, S.M. Gastro-protective effect of *Artemisia Sieberi* essential oil against ethanol-induced ulcer in rats as revealed via biochemical, histopathological and metabolomics analysis. *Biomark. Biochem. Indic. Expo. Response Susceptibility Chem.* **2022**, *27*, 247–257. [[CrossRef](#)] [[PubMed](#)]
14. Kim, D.-S.; Lee, S.; Park, S.M.; Yun, S.H.; Gab, H.-S.; Kim, S.S.; Kim, H.-J. Comparative metabolomics analysis of Citrus varieties. *Foods* **2021**, *10*, 2826. [[CrossRef](#)] [[PubMed](#)]
15. Yao, Z.; Wu, S.; Zhang, H.; Feng, X.; Wang, Z.; Lin, M. Chiral determination of naringenin by ultra-performance liquid chromatography-tandem mass spectrometry and application in Citrus peel and pulp. *Front. Nutr.* **2022**, *9*, 906859. [[CrossRef](#)]
16. Afifi, S.M.; El-Mahis, A.; Heiss, A.G.; Farag, M.A. Gas chromatography-mass spectrometry-based classification of 12 fennel (*Foeniculum vulgare* Miller) varieties based on their aroma profiles and estragole levels as analyzed using chemometric tools. *ACS Omega* **2021**, *6*, 5775–5785. [[CrossRef](#)]
17. El-Newary, S.A.; Afifi, S.M.; Aly, M.S.; Ahmed, R.F.; El Gendy, A.E.-N.G.; Abd-ElGawad, A.M.; Farag, M.A.; Elgamel, A.M.; Elshamy, A.I. Chemical profile of *Launaea nudicaulis* ethanolic extract and its antidiabetic effect in streptozotocin-induced rats. *Molecules* **2021**, *26*, 1000. [[CrossRef](#)]
18. Farag, M.A.; Kabbash, E.M.; Mediani, A.; Döll, S.; Esatbeyoglu, T.; Afifi, S.M. Comparative metabolite fingerprinting of four different cinnamon species analyzed via UPLC-MS and GC-MS and chemometric tools. *Molecules* **2022**, *27*, 2935. [[CrossRef](#)]
19. Ledesma-Escobar, C.; Priego-Capote, F.; Luque de Castro, M. Characterization of lemon (*Citrus limon*) polar extract by liquid chromatography-tandem mass spectrometry in high resolution mode. *J. Mass Spectrom.* **2015**, *50*, 1196–1205. [[CrossRef](#)]
20. Wang, F.; Huang, Y.; Wu, W.; Zhu, C.; Zhang, R.; Chen, J.; Zeng, J. Metabolomics analysis of the peels of different colored citrus fruits (*Citrus reticulata* cv. 'Shatangju') during the maturation period based on UHPLC-QQQ-MS. *Molecules* **2020**, *25*, 396. [[CrossRef](#)]
21. Liu, Y.; Ren, C.; Cao, Y.; Wang, Y.; Duan, W.; Xie, L.; Sun, C.; Li, X. Characterization and purification of bergamottin from *Citrus grandis* (L.) Osbeck cv. Yongjiazaoxiangyou and its antiproliferative activity and effect on glucose consumption in HepG2 cells. *Molecules* **2017**, *22*, 1227. [[CrossRef](#)] [[PubMed](#)]
22. Jo, M.S.; Lee, S.; Yu, J.S.; Baek, S.C.; Cho, Y.-C.; Kim, K.H. Megastigmane derivatives from the cladodes of *Opuntia humifusa* and their nitric oxide inhibitory activities in macrophages. *J. Nat. Prod.* **2020**, *83*, 684–692. [[CrossRef](#)] [[PubMed](#)]
23. Oszmiański, J.; Kolniak-Ostek, J.; Wojdyło, A. Application of ultra performance liquid chromatography-photodiode detector-quadrupole/time of flight-mass spectrometry (UPLC-PDA-Q/TOF-MS) method for the characterization of phenolic compounds of *Lepidium sativum* L. sprouts. *Eur. Food Res. Technol.* **2013**, *236*, 699–706. [[CrossRef](#)]
24. Tine, Y.; Renucci, F.; Costa, J.; Wélé, A.; Paolini, J. A method for LC-MS/MS profiling of coumarins in *Zanthoxylum zanthoxyloides* (Lam.) B. Zepernich and Timler extracts and essential oils. *Molecules* **2017**, *22*, 174. [[CrossRef](#)] [[PubMed](#)]
25. Zagurskaya, Y.V.; Vasil'ev, V.; Bogatyrev, A.; Bayandina, I.; Kukina, T. Flavonoids and hydroxycinnamic acids from *Leonurus quinquelobatus*. *Chem. Nat. Compd.* **2015**, *51*, 156–157. [[CrossRef](#)]
26. Brito, A.; Ramirez, J.E.; Areche, C.; Sepúlveda, B.; Simirgiotis, M.J. HPLC-UV-MS profiles of phenolic compounds and antioxidant activity of fruits from three citrus species consumed in Northern Chile. *Molecules* **2014**, *19*, 17400–17421. [[CrossRef](#)] [[PubMed](#)]
27. Katsuno, T.; Kasuga, H.; Kusano, Y.; Yaguchi, Y.; Tomomura, M.; Cui, J.; Yang, Z.; Baldermann, S.; Nakamura, Y.; Ohnishi, T.; et al. Characterisation of odorant compounds and their biochemical formation in green tea with a low temperature storage process. *Food Chem.* **2014**, *148*, 388–395. [[CrossRef](#)] [[PubMed](#)]
28. Fayek, N.M.; Farag, M.A.; Abdel Monem, A.R.; Moussa, M.Y.; Abd-Elwahab, S.M.; El-Tanbouly, N.D. Comparative metabolite profiling of four citrus peel cultivars via ultra-performance liquid chromatography coupled with quadrupole-time-of-flight-mass spectrometry and multivariate data analyses. *J. Chromatogr. Sci.* **2019**, *57*, 349–360. [[CrossRef](#)] [[PubMed](#)]
29. Cho, H.E.; Ahn, S.Y.; Kim, S.C.; Woo, M.H.; Hong, J.-T.; Moon, D.C. Determination of flavonoid glycosides, polymethoxyflavones, and coumarins in herbal drugs of citrus and poncirus fruits by high performance liquid chromatography-electrospray ionization/tandem mass spectrometry. *Anal. Lett.* **2014**, *47*, 1299–1323. [[CrossRef](#)]
30. Gualdani, R.; Cavalluzzi, M.M.; Lentini, G.; Habtemariam, S. The chemistry and pharmacology of citrus limonoids. *Molecules* **2016**, *21*, 1530. [[CrossRef](#)]
31. Li, K.; Wang, H. Simultaneous determination of matrine, sophoridine and oxymatrine in *Sophora flavescens* Ait. by high performance liquid chromatography. *Biomed. Chromatogr.* **2004**, *18*, 178–182. [[CrossRef](#)]
32. Ding, S.; Zhang, J.; Yang, L.; Wang, X.; Fu, F.; Wang, R.; Zhang, Q.; Shan, Y. Changes in cuticle components and morphology of 'Satsuma' mandarin (*Citrus unshiu*) during ambient storage and their potential role on *Penicillium digitatum* infection. *Molecules* **2020**, *25*, 412. [[CrossRef](#)] [[PubMed](#)]
33. Yang, H.; Tang, Y.; Wang, L.; Guo, Y.; Luo, D.; Wu, L.; Deng, X.; Li, X.; Bai, L. The potential of *Myosoton aquaticum* extracts and compounds to control barnyardgrass (*Echinochloa crus-galli*). *Weed Res.* **2021**, *61*, 317–326. [[CrossRef](#)]

34. Mukai, K.; Takeuchi, M.; Ohnishi, M.; Kudoh, M.; Imai, H. Characterization of ceramides and glucosylceramides of the Satsuma mandarin (*Citrus unshiu*) fruit. *J. Oleo Sci.* **2022**, *71*, 535–540. [[CrossRef](#)] [[PubMed](#)]
35. Ou, M.-C.; Liu, Y.-H.; Sun, Y.-W.; Chan, C.-F. The composition, antioxidant and antibacterial activities of cold-pressed and distilled essential oils of *Citrus paradisi* and *Citrus grandis* (L.) Osbeck. *Evid. -Based Complement. Altern. Med.* **2015**, *2015*, 804091. [[CrossRef](#)] [[PubMed](#)]
36. Dugo, P.; Bonaccorsi, I.; Ragonese, C.; Russo, M.; Donato, P.; Santi, L.; Mondello, L. Analytical characterization of mandarin (*Citrus deliciosa* Ten.) essential oil. *Flavour Fragr. J.* **2011**, *26*, 34–46. [[CrossRef](#)]
37. Lee, S.Y.; Shaari, K. LC–MS metabolomics analysis of *Stevia rebaudiana* Bertoni leaves cultivated in Malaysia in relation to different developmental stages. *Phytochem. Anal.* **2022**, *33*, 249–261. [[CrossRef](#)]
38. Dadwal, V.; Joshi, R.; Gupta, M. A multidimensional UHPLC-DAD-QTOF-IMS gradient approach for qualitative and quantitative investigation of Citrus and Malus fruit phenolic extracts and edibles. *ACS Food Sci. Technol.* **2021**, *1*, 2006–2018. [[CrossRef](#)]
39. Liu, E.H.; Zhao, P.; Duan, L.; Zheng, G.-D.; Guo, L.; Yang, H.; Li, P. Simultaneous determination of six bioactive flavonoids in *Citri Reticulatae Pericarpium* by rapid resolution liquid chromatography coupled with triple quadrupole electrospray tandem mass spectrometry. *Food Chem.* **2013**, *141*, 3977–3983. [[CrossRef](#)]
40. Falcão, S.I.; Vale, N.; Gomes, P.; Domingues, M.R.; Freire, C.; Cardoso, S.M.; Vilas-Boas, M. Phenolic profiling of Portuguese propolis by LC–MS spectrometry: Uncommon propolis rich in flavonoid glycosides. *Phytochem. Anal.* **2013**, *24*, 309–318. [[CrossRef](#)]
41. Shi, Y.-S.; Zhang, Y.; Li, H.-T.; Wu, C.-H.; El-Seedi, H.R.; Ye, W.-K.; Wang, Z.-W.; Li, C.-B.; Zhang, X.-F.; Kai, G.-Y. Limonoids from Citrus: Chemistry, anti-tumor potential, and other bioactivities. *J. Funct. Foods* **2020**, *75*, 104213. [[CrossRef](#)]
42. Tsukayama, M.; Ichikawa, R.; Yamamoto, K.; Sasaki, T.; Kawamura, Y. Microwave-assisted rapid extraction of polymethoxyflavones from dried peels of *Citrus yuko* Hort. ex Tanaka. *Nippon. Shokuhin Kagaku Kogaku Kaishi = J. Jpn. Soc. Food Sci. Technol.* **2009**, *56*, 359–362. [[CrossRef](#)]
43. Lu, V.; Bastaki, M.; Api, A.M.; Aubanel, M.; Bauter, M.; Cachet, T.; Demyttenaere, J.; Diop, M.M.; Harman, C.L.; Hayashi, S.-m.; et al. Dietary administration of β -ionone epoxide to Sprague-Dawley rats for 90 days. *Curr. Res. Toxicol.* **2021**, *2*, 192–201. [[CrossRef](#)]
44. Li, S.; Jiang, Z.; Thamm, L.; Zhou, G. 10-Hydroxy-2-decenoic acid as an antimicrobial agent in draft keg-conditioned wheat beer. *J. Am. Soc. Brew. Chem.* **2010**, *68*, 114–118. [[CrossRef](#)]
45. Yang, M.; Jiang, Z.; Wen, M.; Wu, Z.; Zha, M.; Xu, W.; Zhang, L. Chemical variation of Chenpi (Citrus peels) and corresponding correlated bioactive compounds by LC-MS metabolomics and multibioassay analysis. *Front. Nutr.* **2022**, *9*, 825381. [[CrossRef](#)] [[PubMed](#)]
46. Takiyama, M.; Matsumoto, T.; Watanabe, J. LC-MS/MS detection of citrus unshiu peel-derived flavonoids in the plasma and brain after oral administration of yokukansankachimpihange in rats. *Xenobiotica* **2019**, *49*, 1494–1503. [[CrossRef](#)] [[PubMed](#)]
47. Vukics, V.; Guttman, A. Structural characterization of flavonoid glycosides by multi-stage mass spectrometry. *Mass Spectrom. Rev.* **2010**, *29*, 1–16. [[CrossRef](#)]
48. Lim, T.K. (Ed.) Citrus \times aurantium sweet orange group. In *Edible Medicinal and Non-Medicinal Plants: Volume 4, Fruits*; Springer: Dordrecht, The Netherlands, 2012; pp. 806–831.
49. Ganeshpurkar, A.; Saluja, A. The pharmacological potential of hesperidin. *Indian J. Biochem. Biophys. (IJBB)* **2019**, *56*, 287–300.
50. Zhang, J.-Y.; Li, N.; Che, Y.-Y.; Zhang, Y.; Liang, S.-X.; Zhao, M.-B.; Jiang, Y.; Tu, P.-F. Characterization of seventy polymethoxylated flavonoids (PMFs) in the leaves of *Murraya paniculata* by on-line high-performance liquid chromatography coupled to photodiode array detection and electrospray tandem mass spectrometry. *J. Pharm. Biomed. Anal.* **2011**, *56*, 950–961. [[CrossRef](#)]
51. Fattahi, M.; Cusido, R.M.; Khojasteh, A.; Bonfill, M.; Palazon, J. Xanthomicrol: A comprehensive review of its chemistry, distribution, biosynthesis and pharmacological activity. *Mini Rev. Med. Chem.* **2014**, *14*, 725–733. [[CrossRef](#)]
52. Gao, Z.; Gao, W.; Zeng, S.-L.; Li, P.; Liu, E.H. Chemical structures, bioactivities and molecular mechanisms of citrus polymethoxyflavones. *J. Funct. Foods* **2018**, *40*, 498–509. [[CrossRef](#)]
53. Lai, C.-S.; Wu, J.-C.; Ho, C.-T.; Pan, M.-H. Disease chemopreventive effects and molecular mechanisms of hydroxylated polymethoxyflavones. *BioFactors* **2015**, *41*, 301–313. [[CrossRef](#)] [[PubMed](#)]
54. Tundis, R.; Loizzo, M.R.; Menichini, F. An overview on chemical aspects and potential health benefits of limonoids and their derivatives. *Crit. Rev. Food Sci. Nutr.* **2014**, *54*, 225–250. [[CrossRef](#)]
55. Russo, M.; Arigò, A.; Calabrò, M.L.; Farnetti, S.; Mondello, L.; Dugo, P. Bergamot (*Citrus bergamia* Risso) as a source of nutraceuticals: Limonoids and flavonoids. *J. Funct. Foods* **2016**, *20*, 10–19. [[CrossRef](#)]
56. Breksa III, A.P.; Hidalgo, M.B.; Yuen, M.L. Liquid chromatography–electrospray ionisation mass spectrometry method for the rapid identification of citrus limonoid glucosides in citrus juices and extracts. *Food Chem.* **2009**, *117*, 739–744. [[CrossRef](#)]
57. Pessoa, L.G.A.; Pessoa, L.A.; da Silva Santos, É.; Pilau, E.J.; Gonçalves, J.E.; Gonçalves, R.A.C.; de Oliveira, A.J.B. Limonoid detection and profile in callus culture of sweet orange. *Acta Scientiarum. Biol. Sci.* **2021**, *43*, e53075. [[CrossRef](#)]
58. Vu, T.O.; Seo, W.; Lee, J.H.; Min, B.S.; Kim, J.A. Terpenoids from *Citrus unshiu* peels and their effects on NO production. *Nat. Prod. Sci.* **2020**, *26*, 176–181.
59. Wedamulla, N.E.; Fan, M.; Choi, Y.-J.; Kim, E.-K. Citrus peel as a renewable bioresource: Transforming waste to food additives. *J. Funct. Foods* **2022**, *95*, 105163. [[CrossRef](#)]
60. Dembitsky, V.M.; Maoka, T. Allenic and cumulenenic lipids. *Prog. Lipid Res.* **2007**, *46*, 328–375. [[CrossRef](#)] [[PubMed](#)]

61. Takita, M.A.; Berger, I.J.; Basílio-Palmieri, A.C.; Borges, K.M.; Souza, J.M.d.; Targon, M.L. Terpene production in the peel of sweet orange fruits. *Genet. Mol. Biol.* **2007**, *30*, 841–847. [[CrossRef](#)]
62. Farag, M.A.; Afifi, S.M.; Rasheed, D.M.; Khattab, A.R. Revealing compositional attributes of *Glossostemon bruguieri* Desf. root geographic origin and roasting impact via chemometric modeling of SPME-GC-MS and NMR metabolite profiles. *J. Food Compos. Anal.* **2021**, *102*, 104073. [[CrossRef](#)]
63. Ammar, N.M.; Hassan, H.A.; Abdallah, H.M.I.; Afifi, S.M.; Elgamal, A.M.; Farrag, A.R.H.; El-Gendy, A.E.-N.G.; Farag, M.A.; Elshamy, A.I. Protective effects of naringenin from *Citrus sinensis* (var. Valencia) peels against CCl₄-induced hepatic and renal injuries in rats assessed by metabolomics, histological and biochemical analyses. *Nutrients* **2022**, *14*, 841. [[CrossRef](#)] [[PubMed](#)]
64. Farag, M.A.; Khattab, A.R.; Shamma, S.; Afifi, S.M. Profiling of primary metabolites and volatile determinants in mahlab cherry (*Prunus mahaleb* L.) seeds in the context of its different varieties and roasting as analyzed using chemometric tools. *Foods* **2021**, *10*, 728. [[CrossRef](#)] [[PubMed](#)]

Disclaimer/Publisher’s Note: The statements, opinions and data contained in all publications are solely those of the individual author(s) and contributor(s) and not of MDPI and/or the editor(s). MDPI and/or the editor(s) disclaim responsibility for any injury to people or property resulting from any ideas, methods, instructions or products referred to in the content.